Tailoring the structures and gas adsorption properties of copper-bent diisophthalate frameworks by substituent-driven ligand conformation regulation strategy

Minghui He, Xiaoxia Gao, Tingting Xu, Zhenzhen Jiang, and Yabing He*

Key Laboratory of the Ministry of Education for Advanced Catalysis Materials, College of Chemistry and Life Sciences, Zhejiang Normal University, Jinhua 321004, China. E-mail: heyabing@zjnu.cn

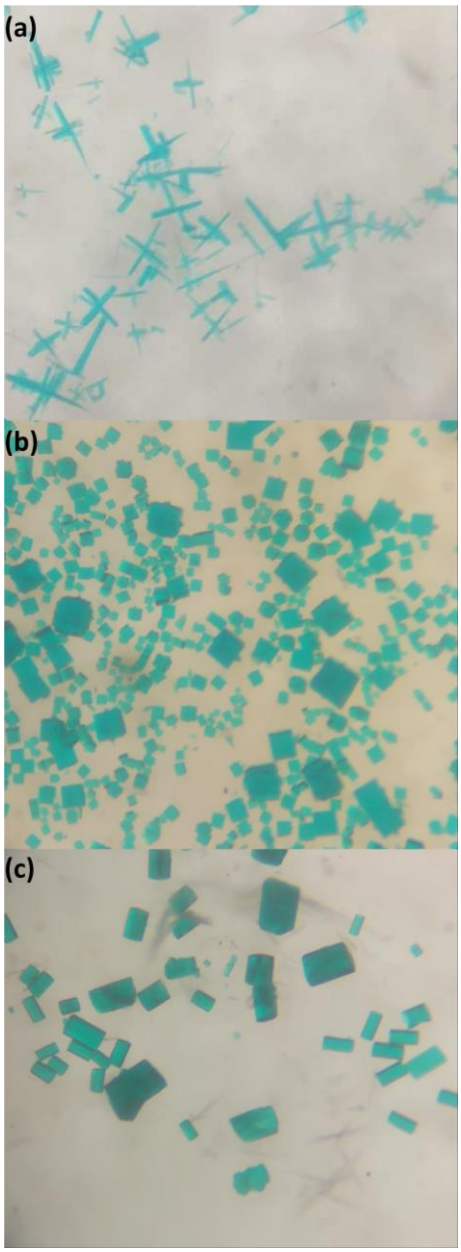

Fig. S1 Electronic photographs of (a) **ZJNU-101**, (b) **ZJNU-102**, and (c) **ZJNU-103**.

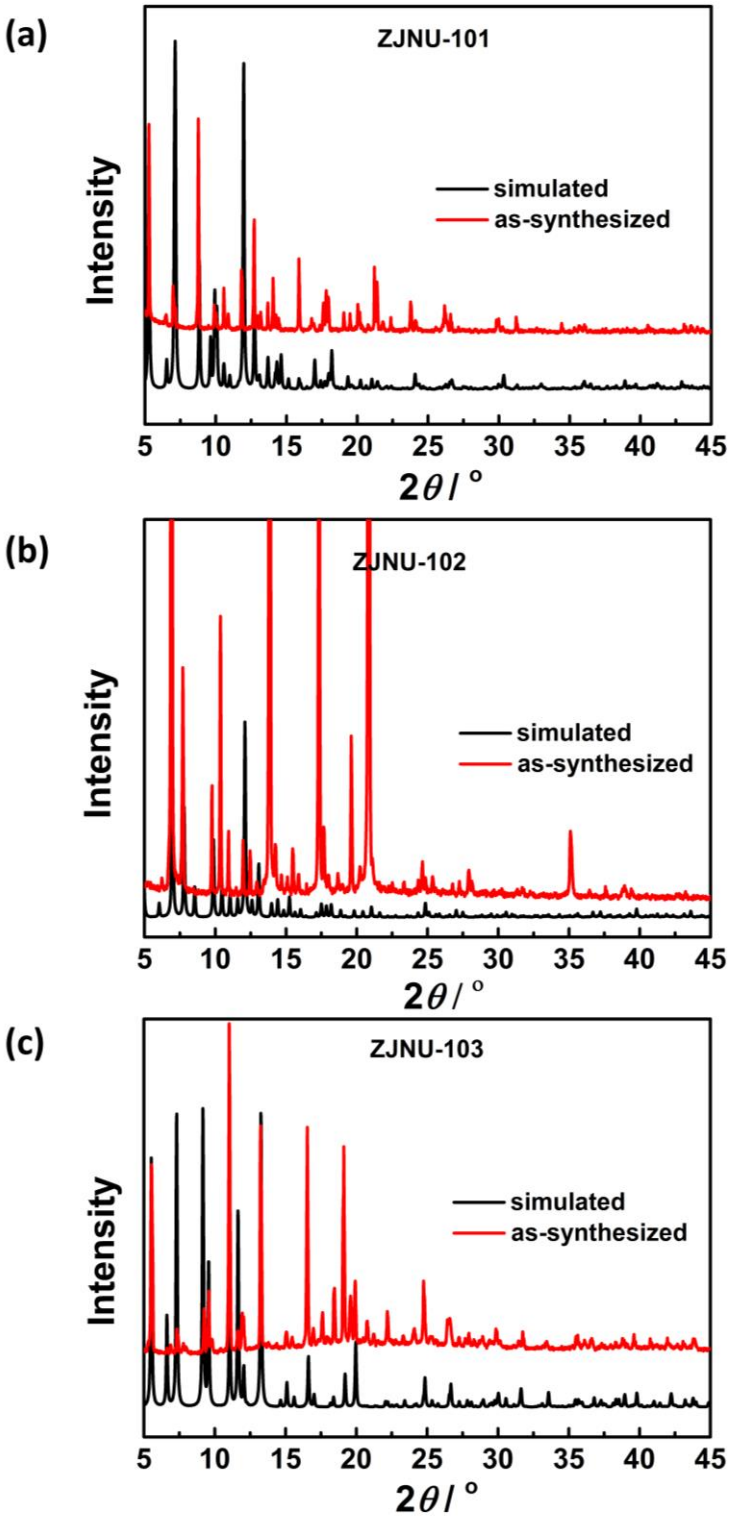

Fig. S2 Comparison of the simulated (black) and experimental (red) PXRD patterns of (a) **ZJNU-101**, (b) **ZJNU-102**, and (c) **ZJNU-103**.

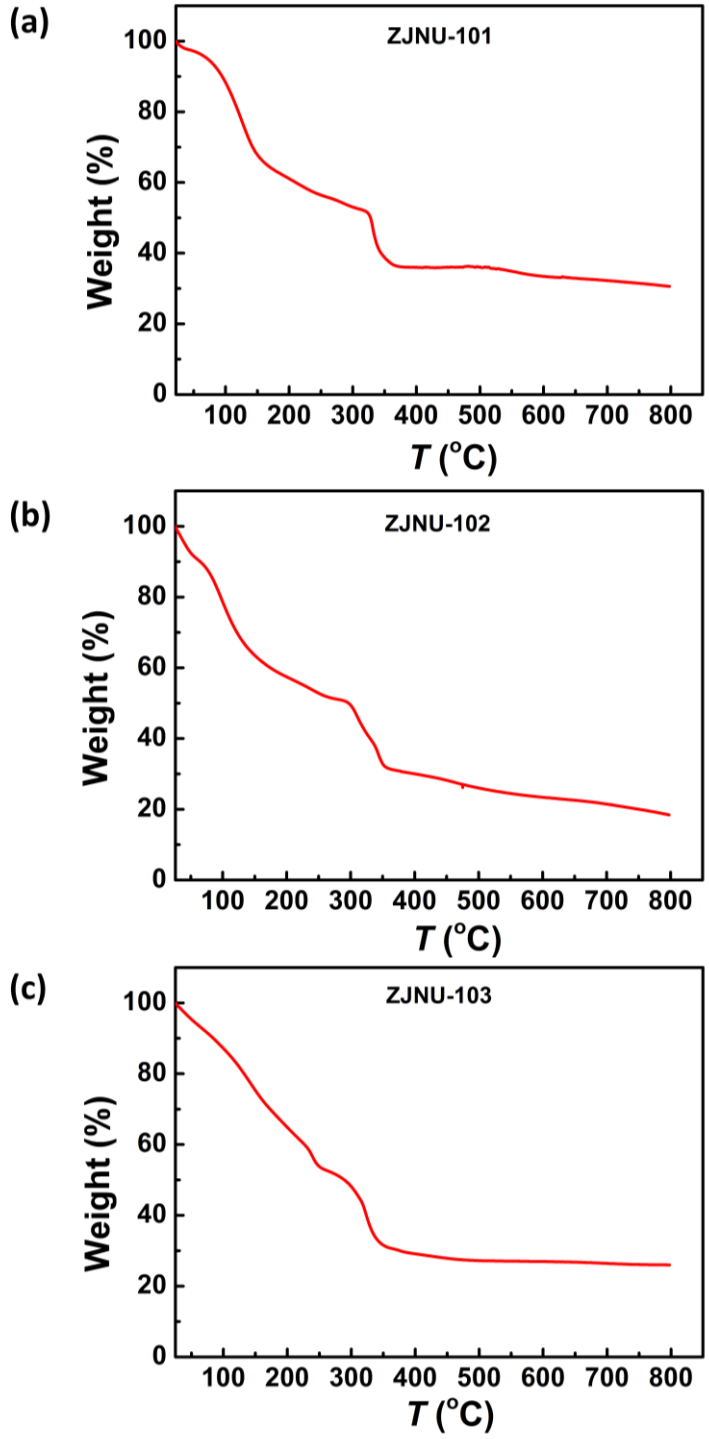

Fig. S3 TGA curves of (a) **ZJNU-101**, (b) **ZJNU-102**, and (c) **ZJNU-103** under N_2 atmosphere.

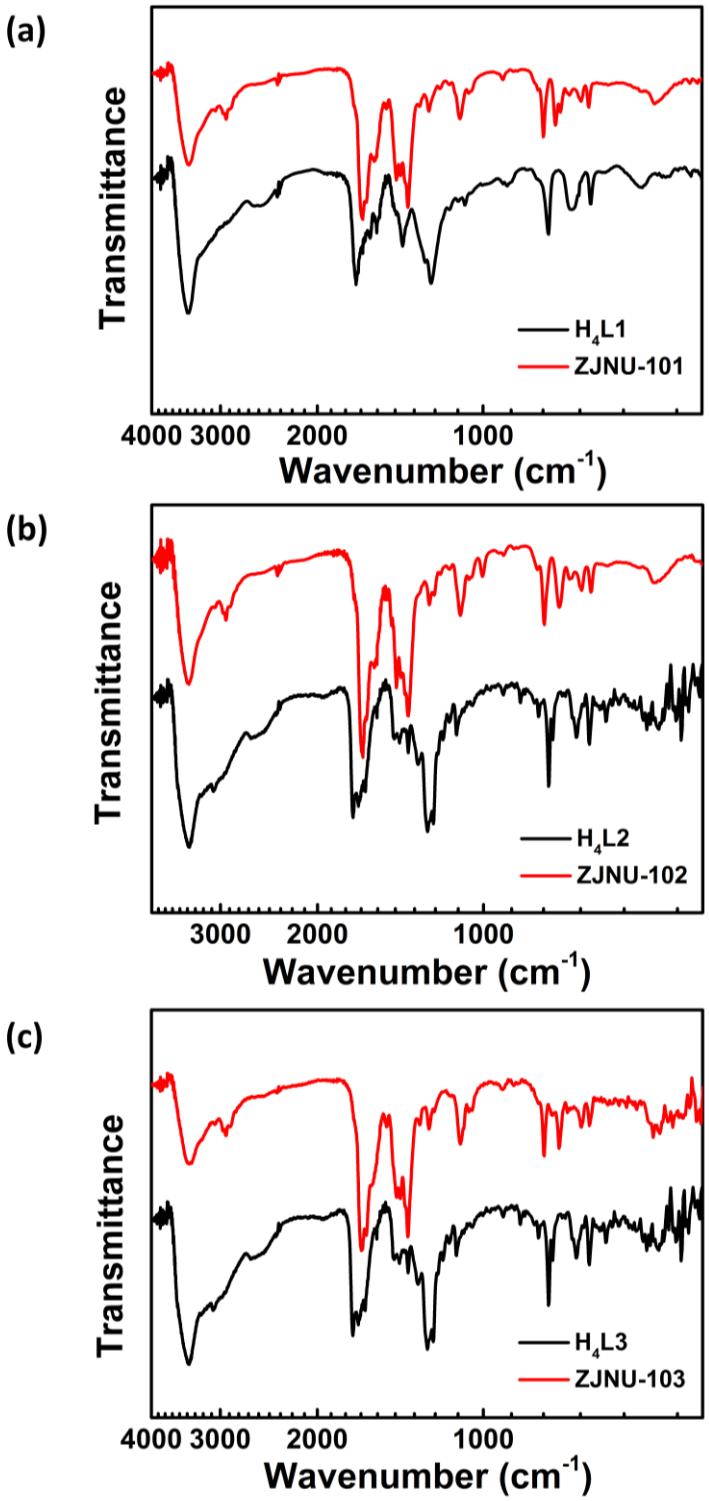

Fig. S4 Comparison of FTIR spectra of (a) **ZJNU-101** and its corresponding ligand H_4L1, (b) **ZJNU-102** and its corresponding ligand H_4L2, and (c) **ZJNU-103** and its corresponding ligand H_4L3.

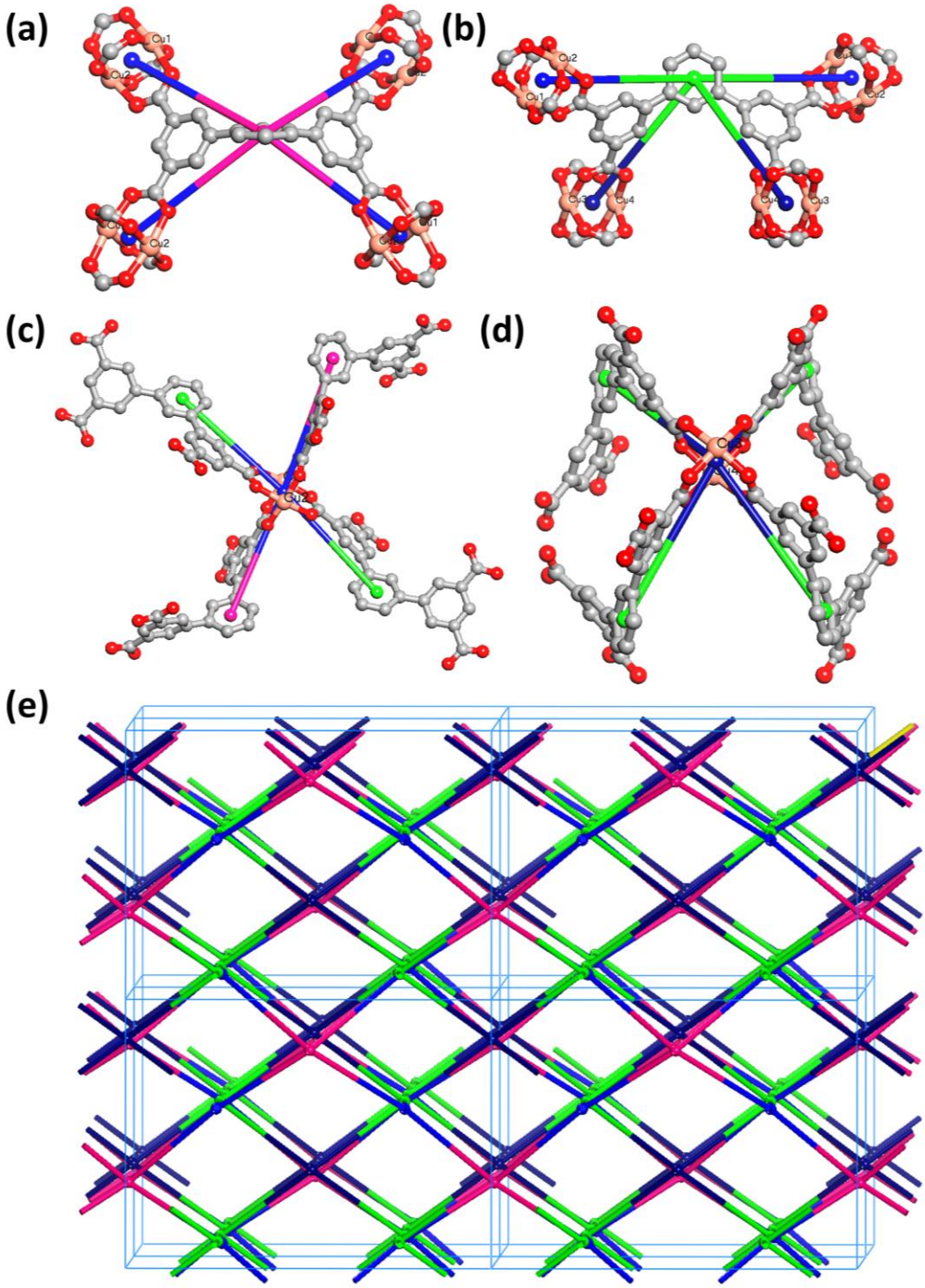

Fig. S5 Topological structural analyses of **ZJNU-101**.

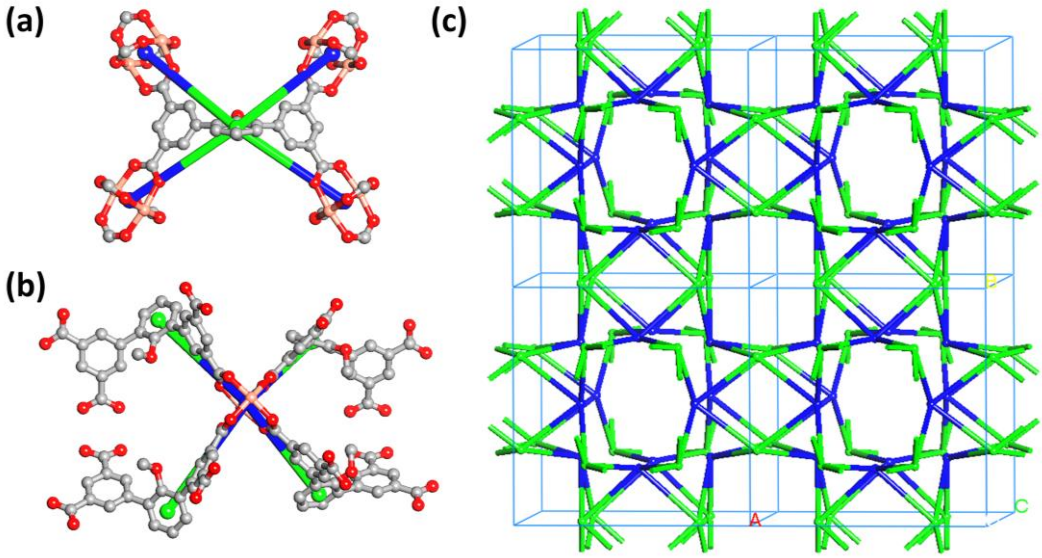

Fig. S6 Topological structural analyses of **ZJNU-102**.

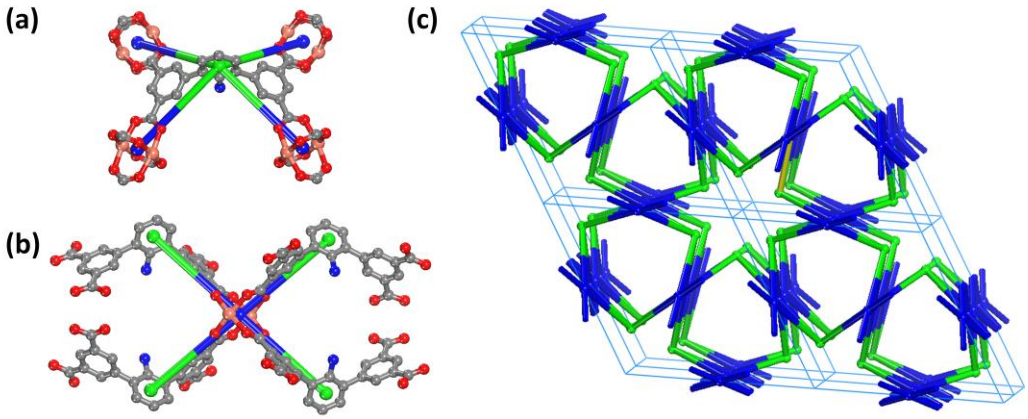

Fig. S7 Topological structural analyses of **ZJNU-103**.

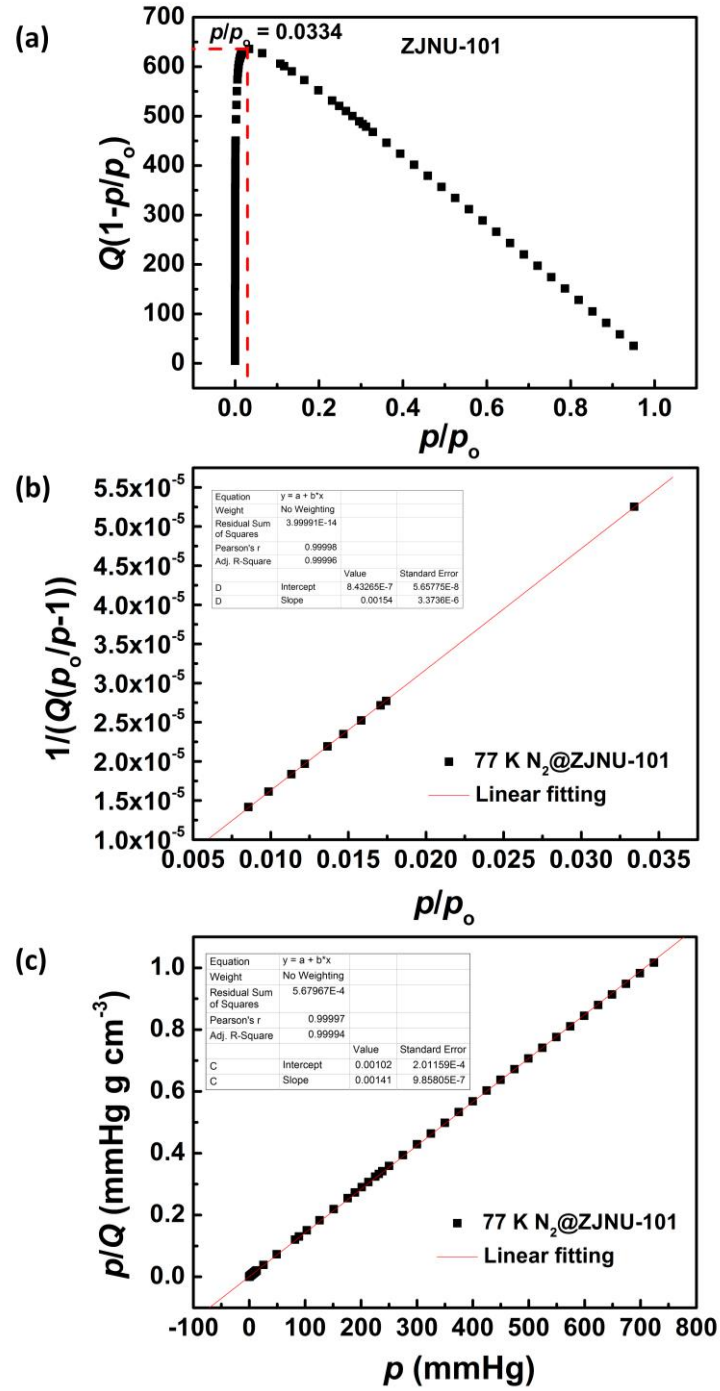

S_{BET} = 1/(8.43265×10^{-7}+ 0.00154)/22414 × 6.023 × 10^{23} × 0.162 × 10^{-18} = 2825 m^2 g^{-1}

$S_{Langmuir}$= (1/0.00141)/22414 × 6.023 × 10^{23} × 0.162 × 10^{-18} = 3087 m^2 g^{-1}

BET constant C = 1 + 0.00154/8.43265×10^{-7} = 1827

$$(p/p_o)_{n_m} = \frac{1}{\sqrt{C}+1} = 0.02286$$

Fig. S8 The consistency plot (a), BET surface area plot (b), and Langmuir surface area plot (c) for **ZJNU-101**.

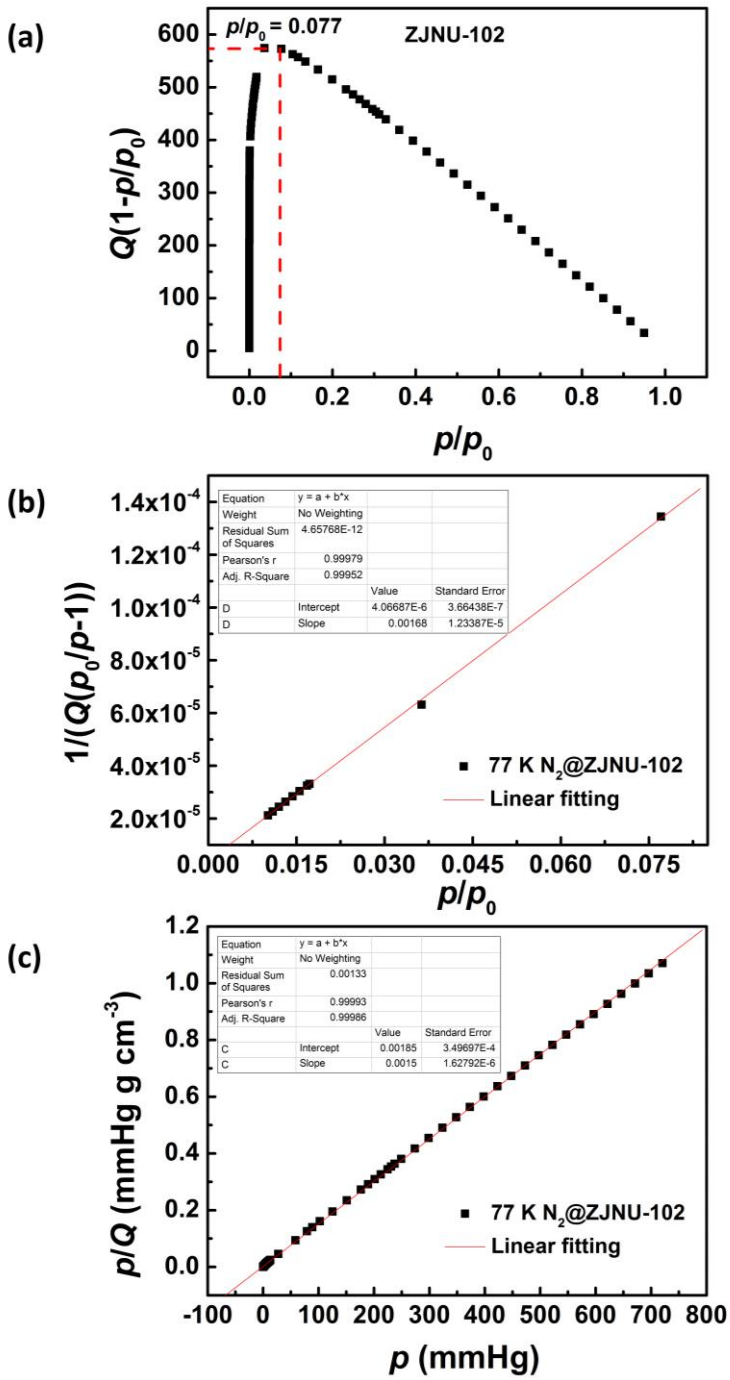

S_{BET} = 1/(4.06687 ×10^{-6} + 0.00168)/22414 × 6.023 × 10^{23} × 0.162 × 10^{-18} = 2585 m^2 g^{-1}

$S_{Langmuir}$= (1/0.0015)/22414 × 6.023 × 10^{23} × 0.162 × 10^{-18} = 2902 m^2 g^{-1}

BET constant C = 1 + 0.00168/4.06687 ×10^{-6} = 414

$$(p/p_o)_{n_m} = \frac{1}{\sqrt{C}+1} = 0.04684$$

Fig. S9 (a) The consistency plot, (b) BET surface area plot, and (c) Langmuir surface area plot for **ZJNU-102**.

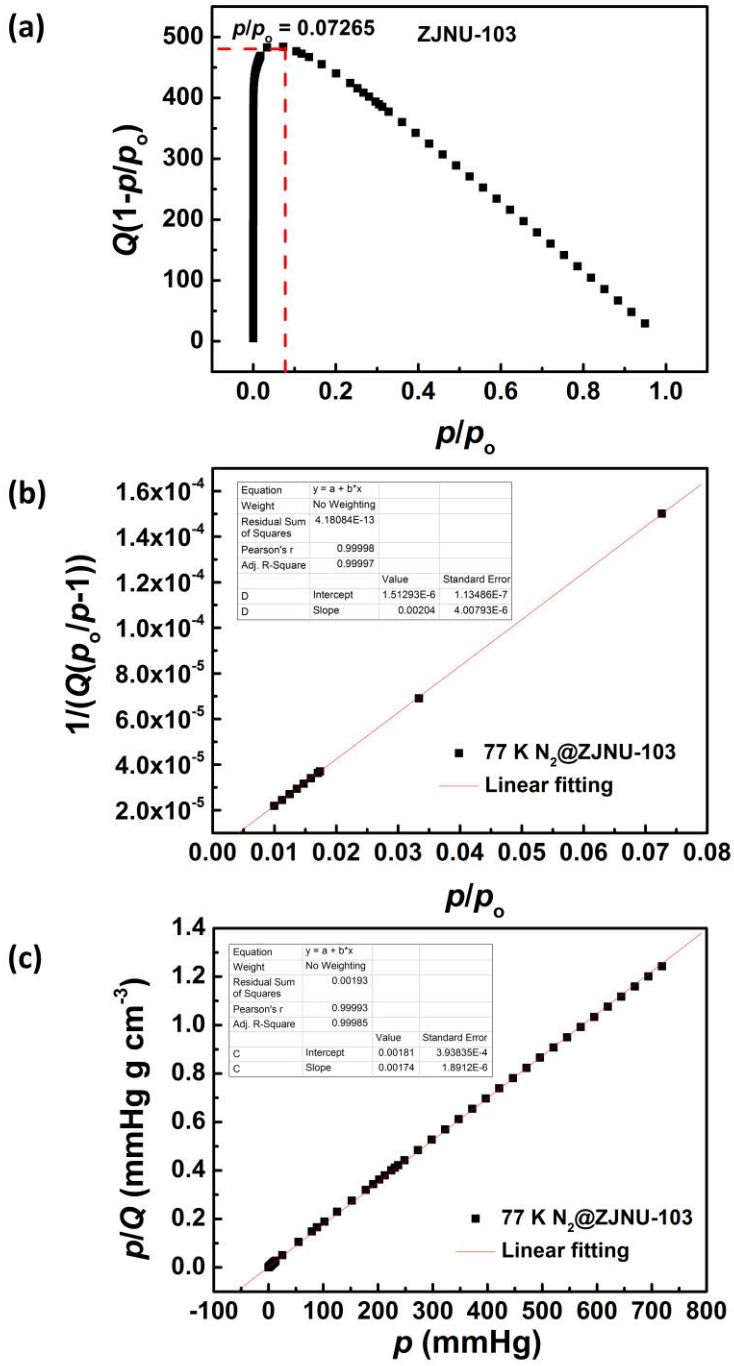

S_{BET} = 1/(1.51293×10^{-6} + 0.00204)/22414 × 6.023 × 10^{23} × 0.162 × 10^{-18} = 2132 m^2 g^{-1}

$S_{Langmuir}$= (1/0.00174)/22414 × 6.023 × 10^{23} × 0.162 × 10^{-18} = 2502 m^2 g^{-1}

BET constant C = 1 + 0.00204/1.51293×10^{-6} = 1349

$$(p/p_o)_{n_m} = \frac{1}{\sqrt{C}+1} = 0.0265$$

Fig. S10 (a) The consistency plot, (b) BET surface area plot, and (c) Langmuir surface area plot for **ZJNU-103**.

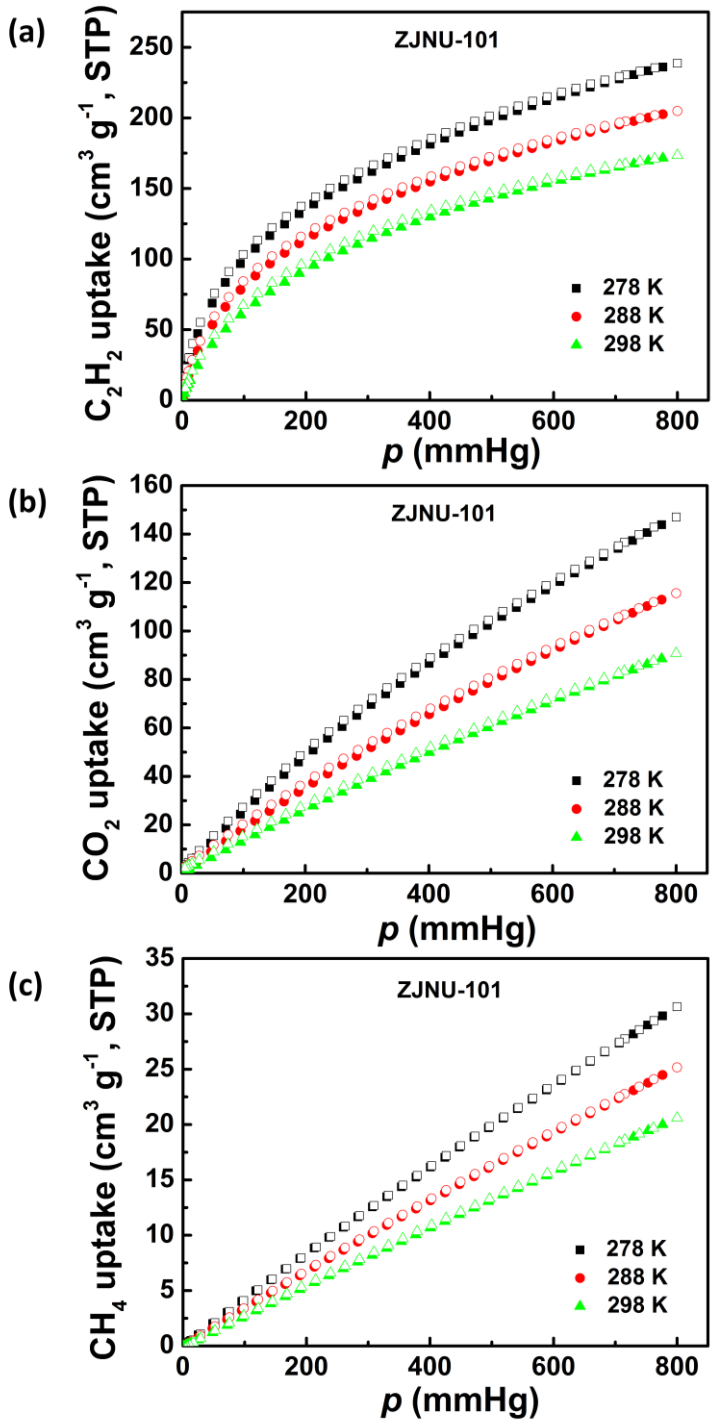

Fig. S11 (a) C_2H_2, (b) CO_2, and (c) CH_4 isotherms of **ZJNU-101** at three different temperatures of 278 K, 288 K, and 298 K. The solid and open symbols represent adsorption and desorption, respectively.

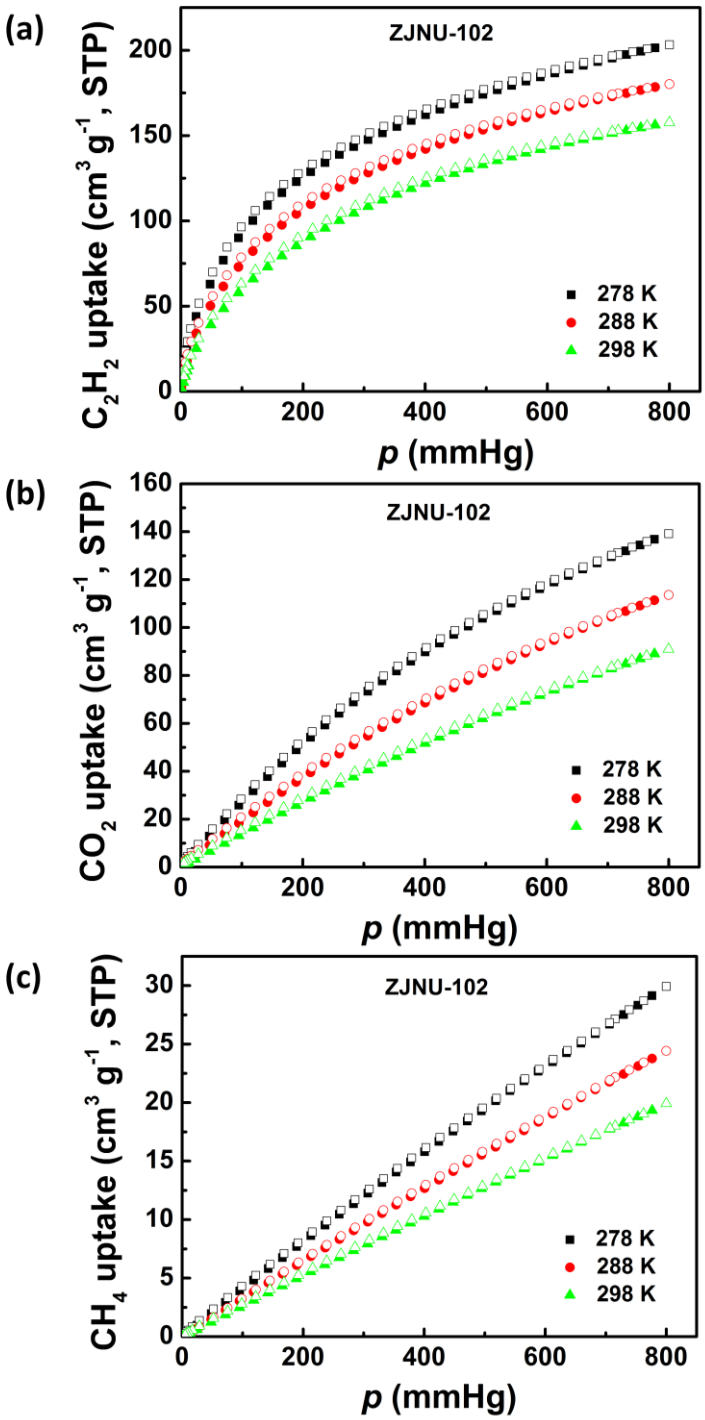

Fig. S12 (a) C_2H_2, (b) CO_2, and (c) CH_4 isotherms of **ZJNU-102** at three different temperatures of 278 K, 288 K, and 298 K. The solid and open symbols represent adsorption and desorption, respectively.

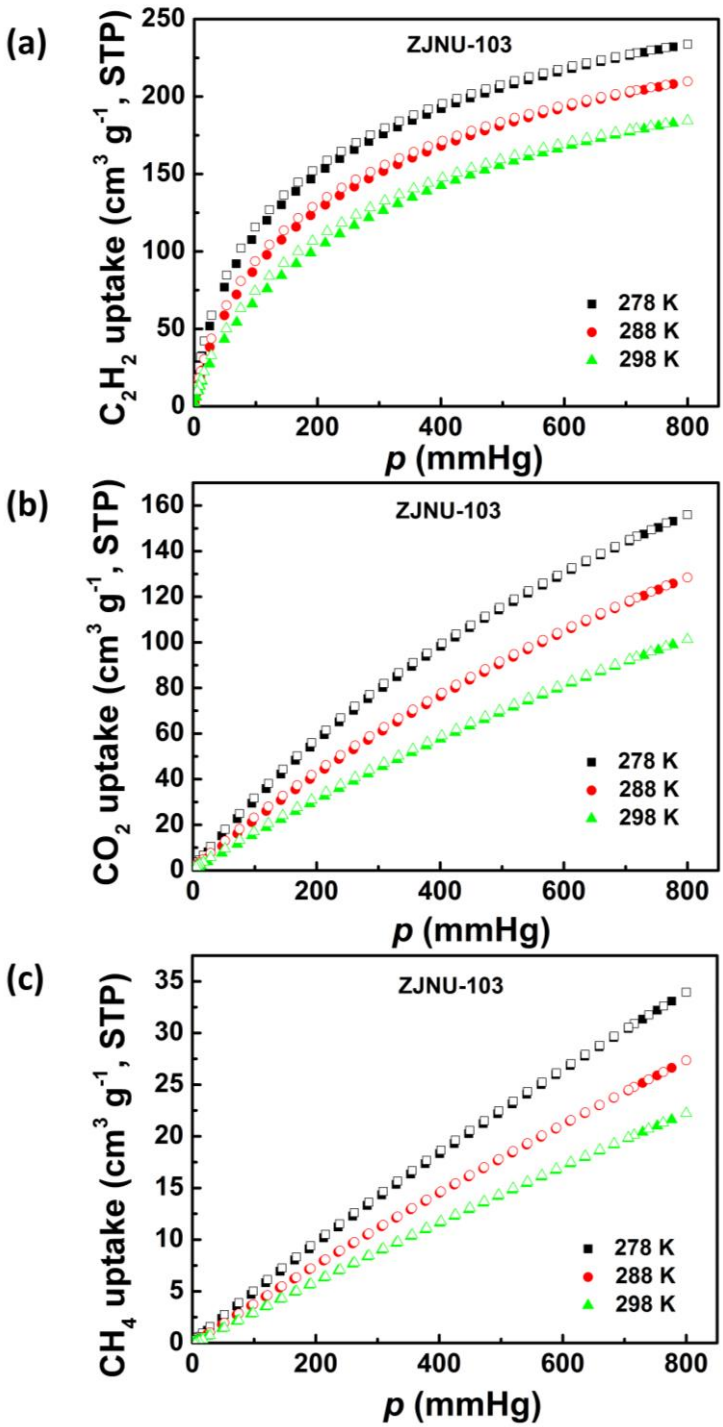

Fig. S13 (a) C_2H_2, (b) CO_2, and (c) CH_4 isotherms of **ZJNU-103** at three different temperatures of 278 K, 288 K, and 298 K. The solid and open symbols represent adsorption and desorption, respectively.

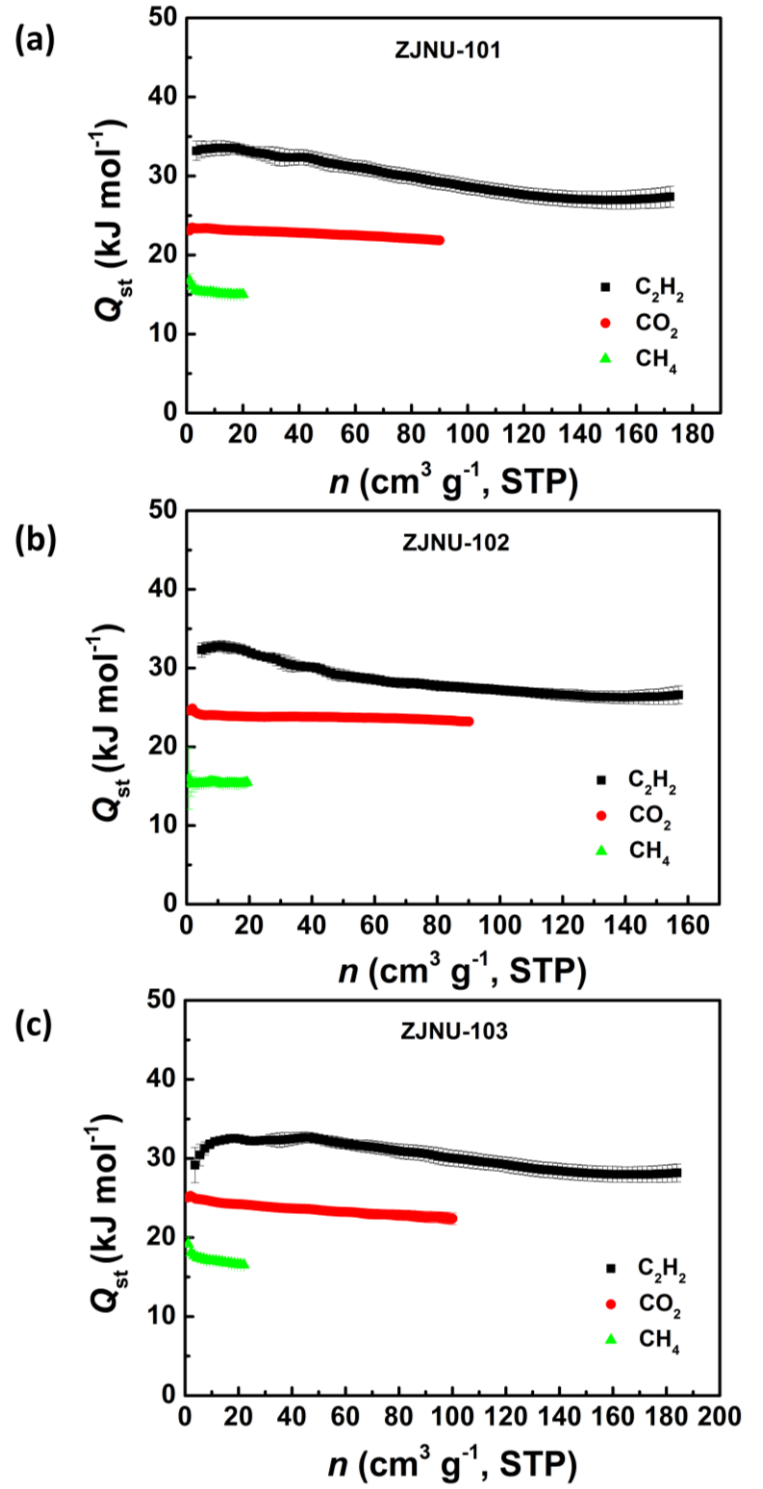

Fig. S14 The isosteric heat of C_2H_2, CO_2, and CH_4 adsorption in (a) **ZJNU-101**, (b) **ZJNU-102**, and (c) **ZJNU-103**.

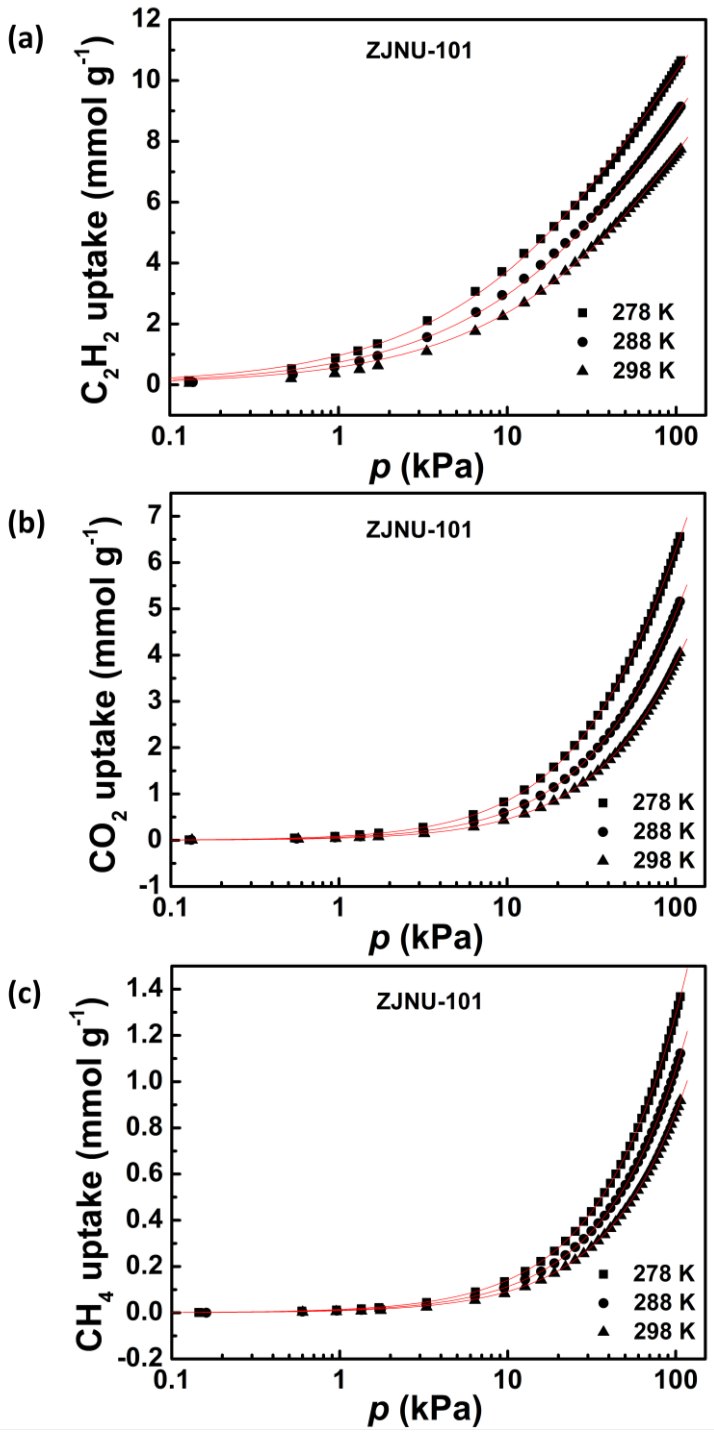

Fig. S15 Comparison of the pure-component isotherm data for (a) C_2H_2, (b) CO_2, and (c) CH_4 in **ZJNU-101** with the fitted isotherms at 278 K, 288 K, and 298 K.

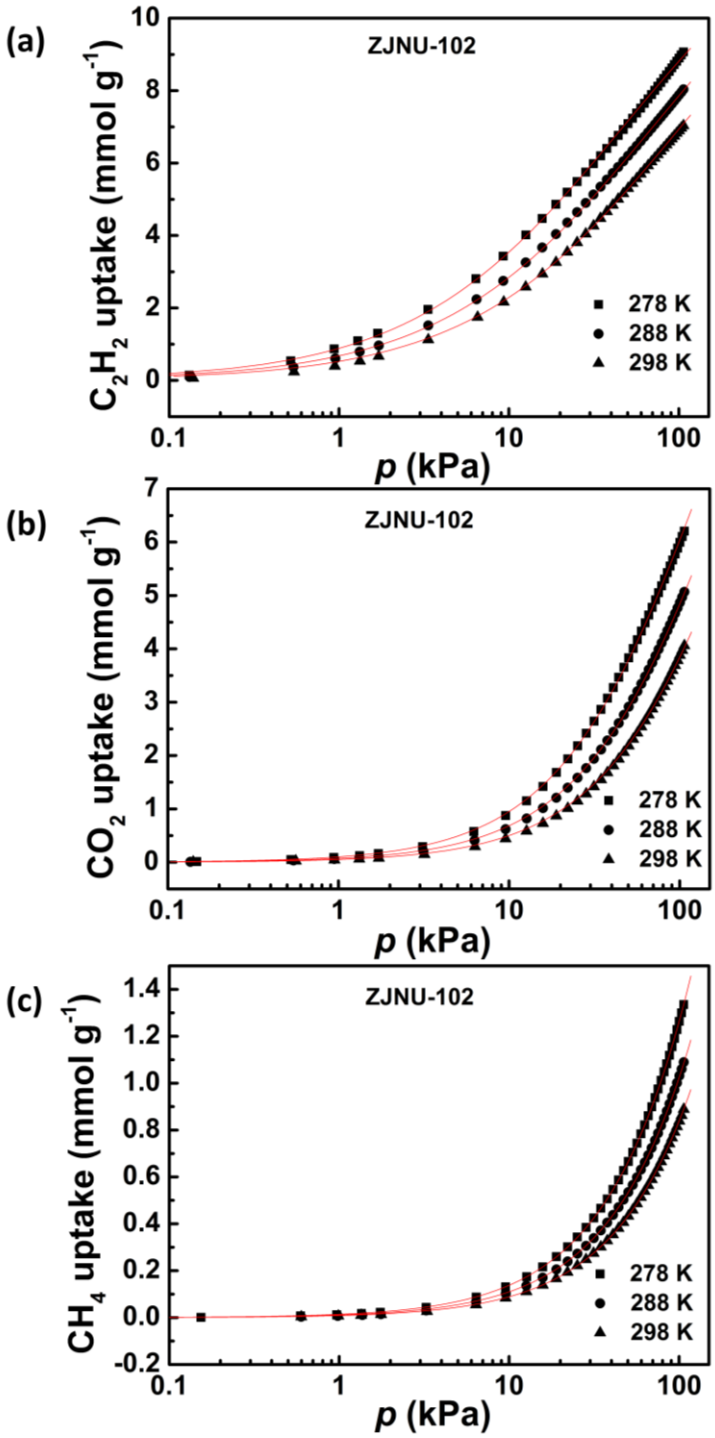

Fig. S16 Comparison of the pure-component isotherm data for (a) C_2H_2, (b) CO_2, and (c) CH_4 in **ZJNU-102** with the fitted isotherms at 278 K, 288 K, and 298 K.

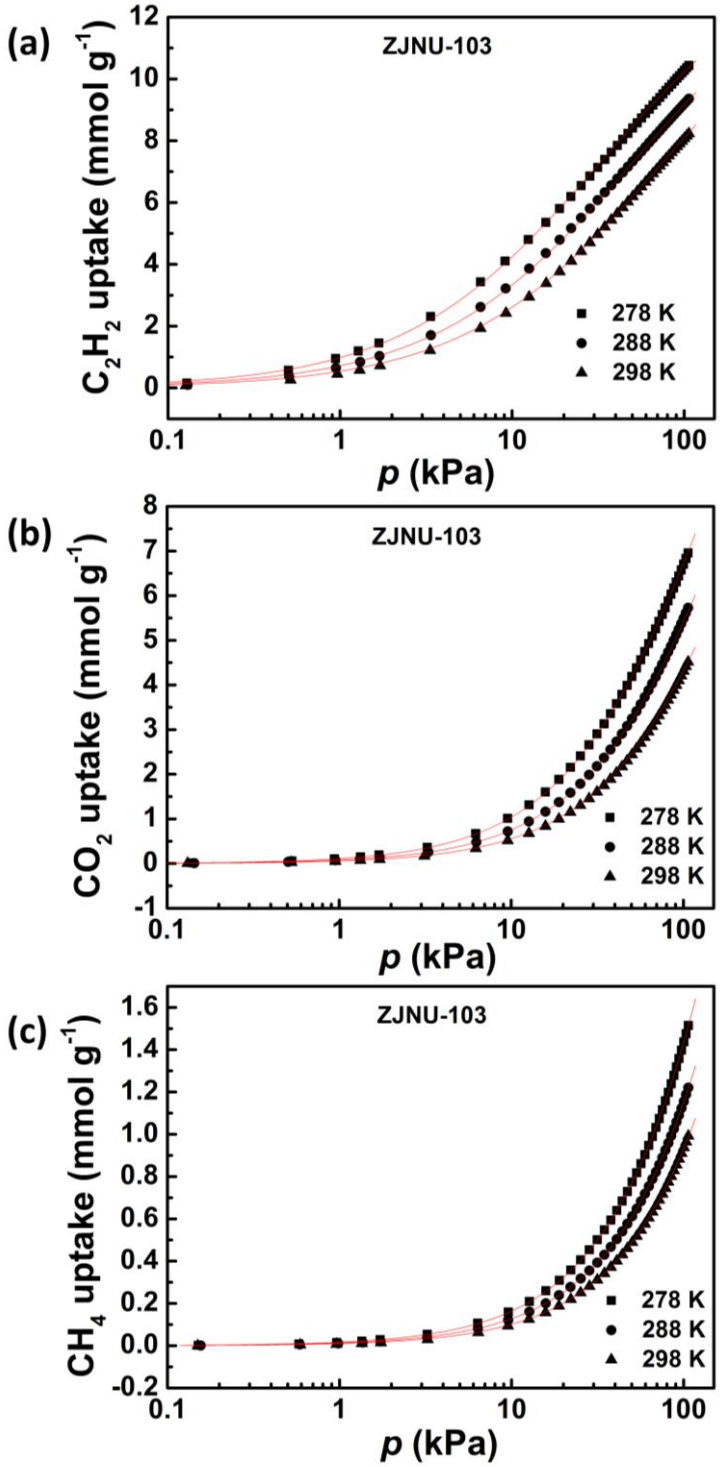

Fig. S17 Comparison of the pure-component isotherm data for (a) C_2H_2, (b) CO_2, and (c) CH_4 in **ZJNU-103** with the fitted isotherms at 278 K, 288 K, and 298 K.

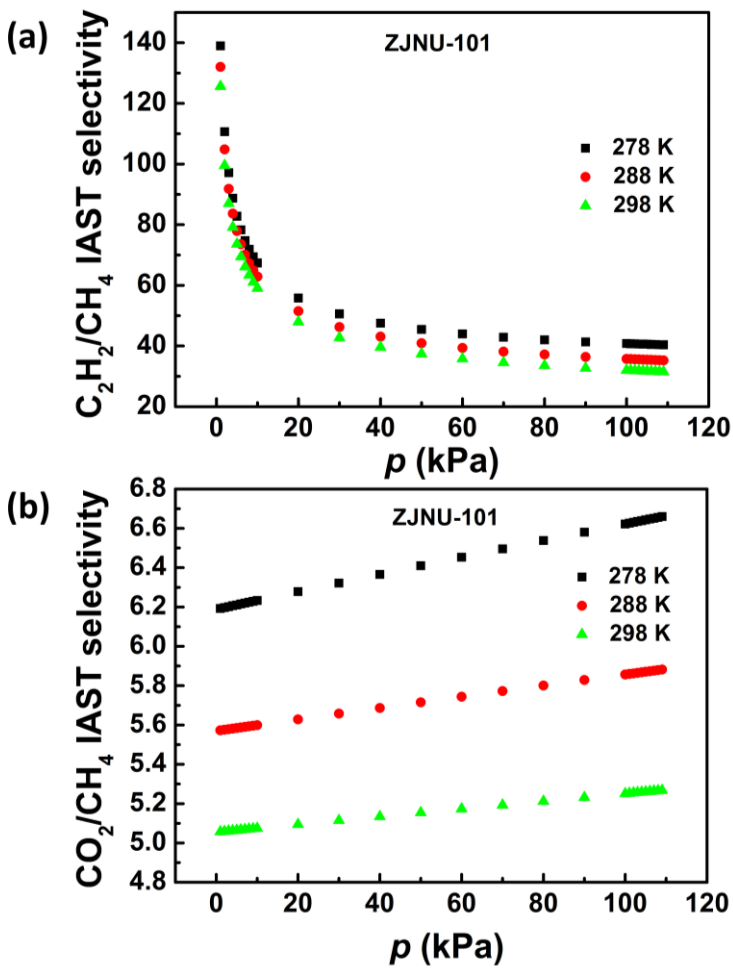

Fig. S18 The IAST-predicted adsorption selectivity for the equimolar (a) C_2H_2-CH_4, and (b) CO_2-CH_4 binary gas mixtures in **ZJNU-101** at three different temperatures of 298 K, 288 K, and 278 K.

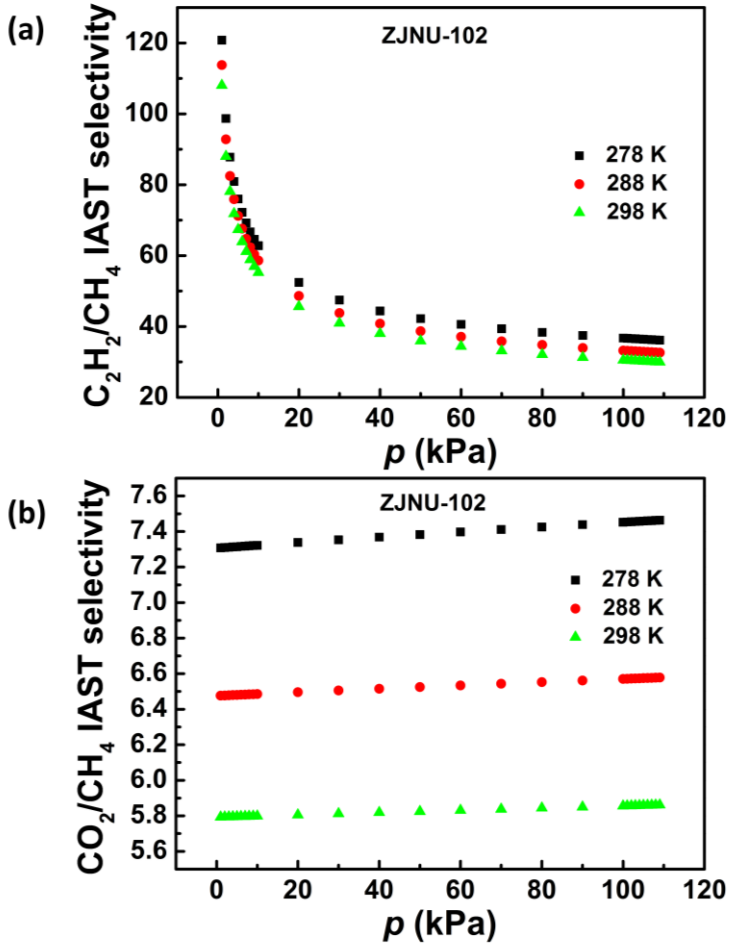

Fig. S19 The IAST-predicted adsorption selectivity for the equimolar (a) C_2H_2-CH_4, and (b) CO_2-CH_4 binary gas mixtures in **ZJNU-102** at three different temperatures of 298 K, 288 K, and 278 K.

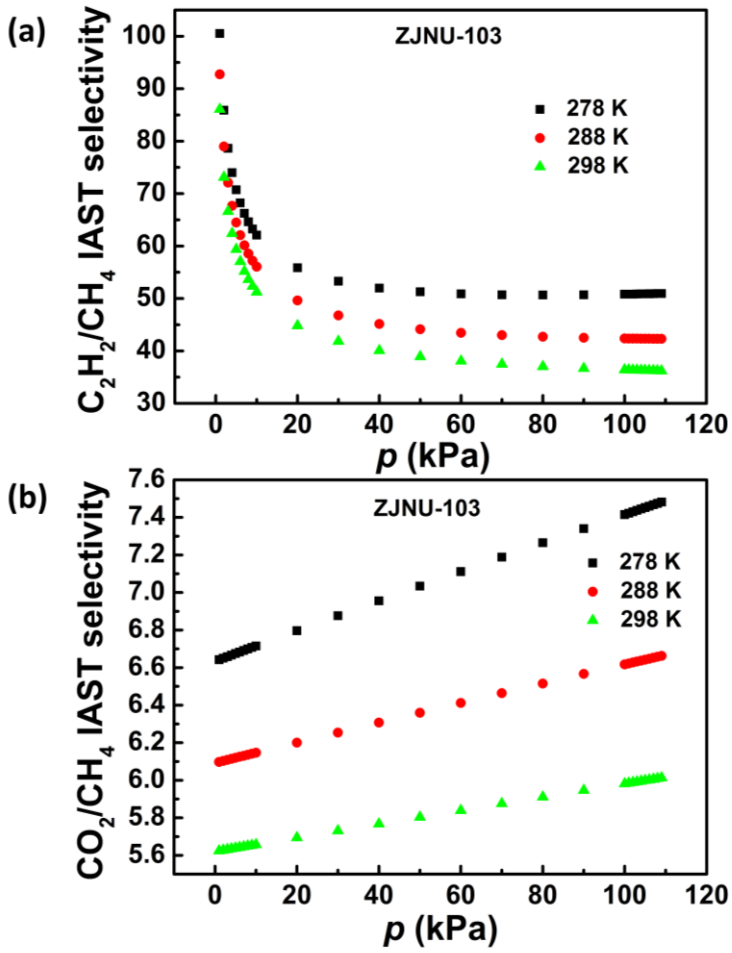

Fig. S20 The IAST-predicted adsorption selectivity for the equimolar (a) C_2H_2-CH_4, and (b) CO_2-CH_4 binary gas mixtures in **ZJNU-103** at three different temperatures of 298 K, 288 K, and 278 K.

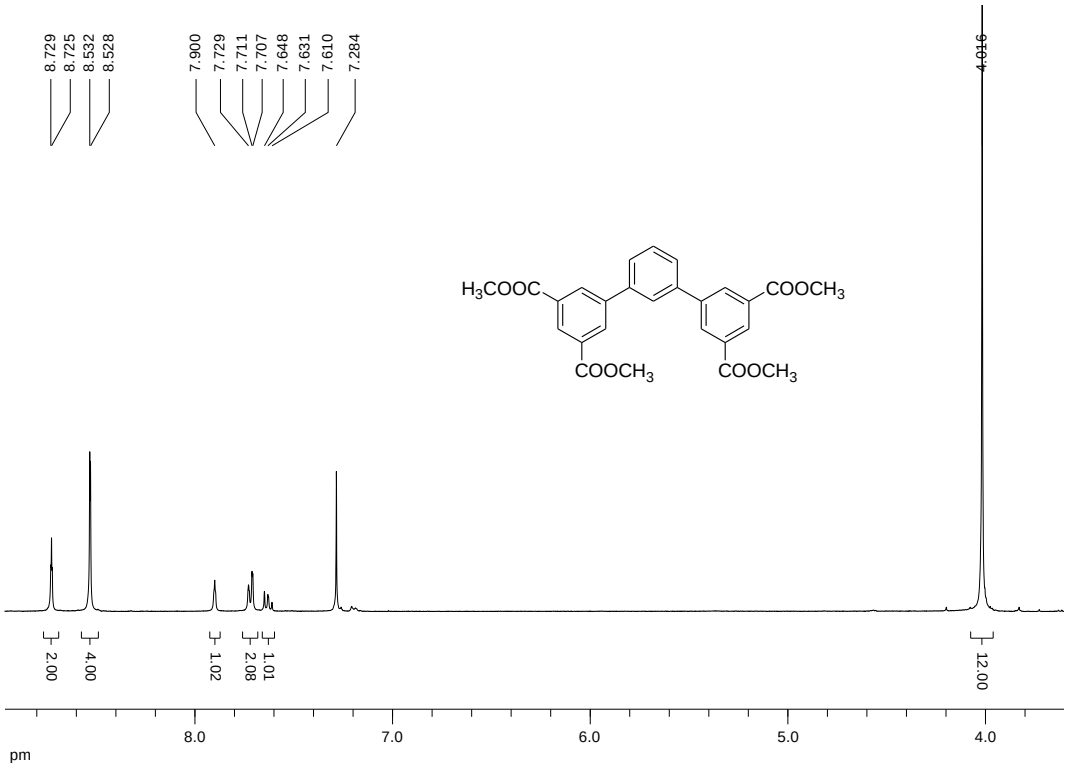
8.729
8.725
8.532
8.528
7.900
7.729
7.711
7.707
7.648
7.631
7.610
7.284
4.016
H3COOC
COOCH3
COOCH3
COOCH3
2.00
4.00
1.02
2.08
1.01
12.00
8.0
7.0
6.0
5.0
4.0
pm

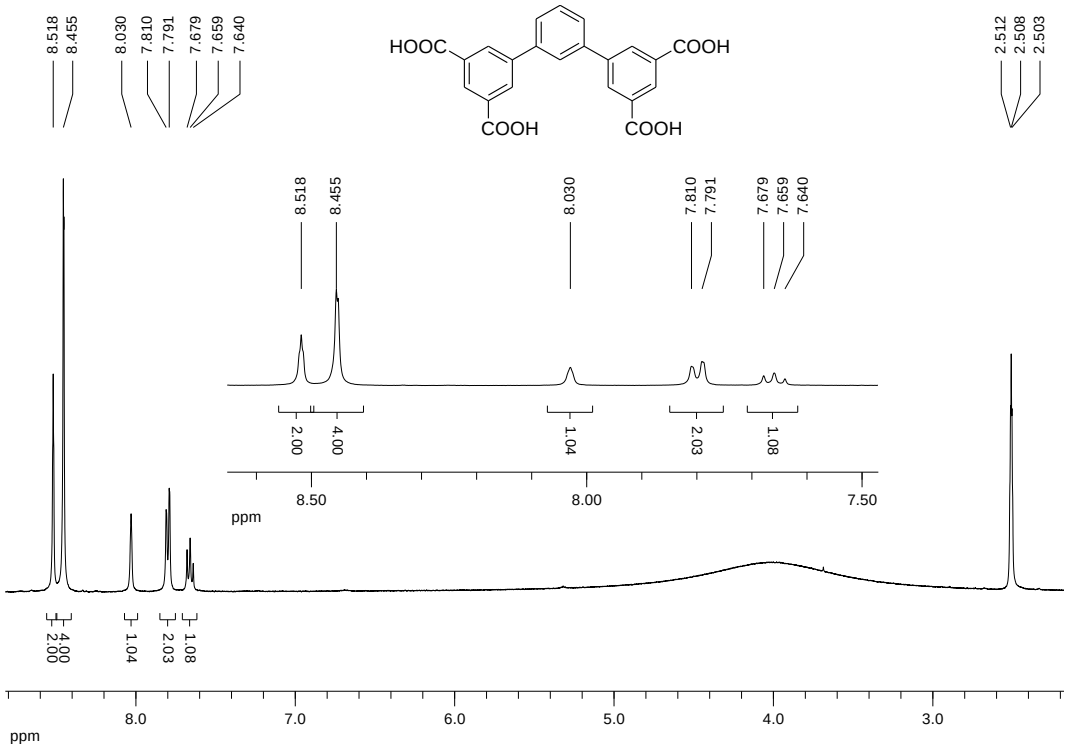
8.518
8.455
8.030
7.810
7.791
7.679
7.659
7.640
HOOC
COOH
COOH
COOH
2.512
2.508
2.503
2.00
4.00
1.04
2.03
1.08
8.50
8.00
7.50
ppm
4.00
2.00
1.04
2.03
1.08
8.0
7.0
6.0
5.0
4.0
3.0
ppm

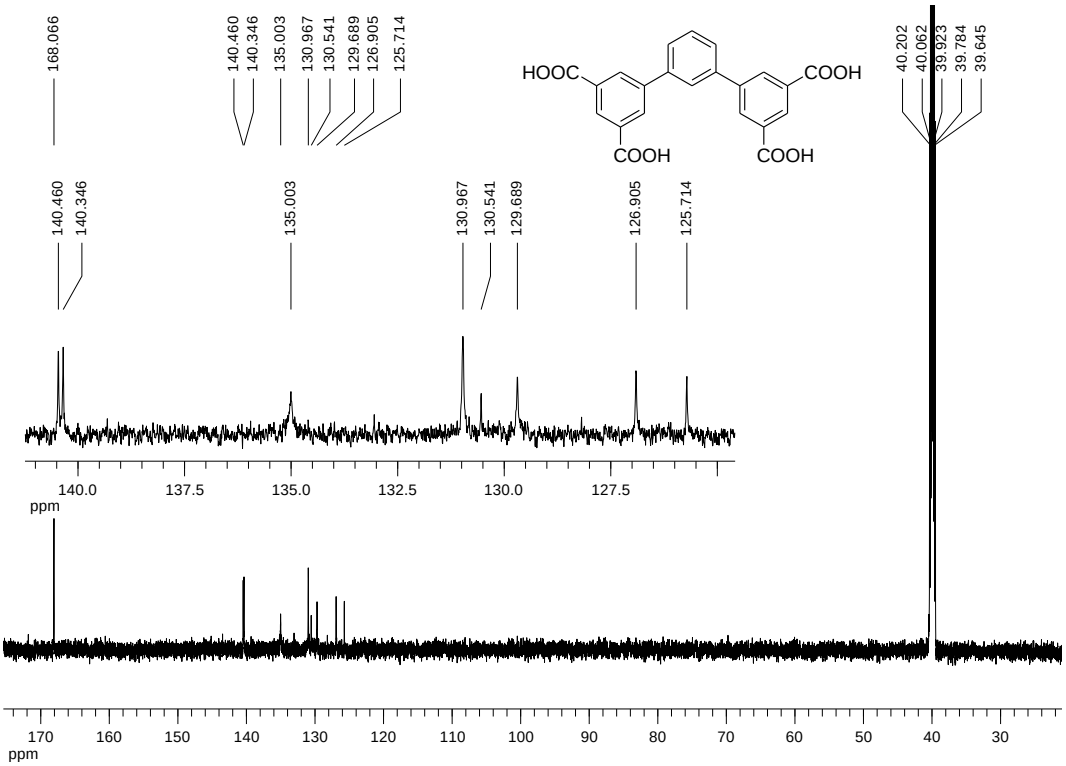
168.066
140.460
140.346
135.003
130.967
130.541
129.689
126.905
125.714
HOOC
COOH
COOH
COOH
40.202
40.062
39.923
39.784
39.645
140.0
137.5
135.0
132.5
130.0
127.5
ppm
170
160
150
140
130
120
110
100
90
80
70
60
50
40
30
ppm

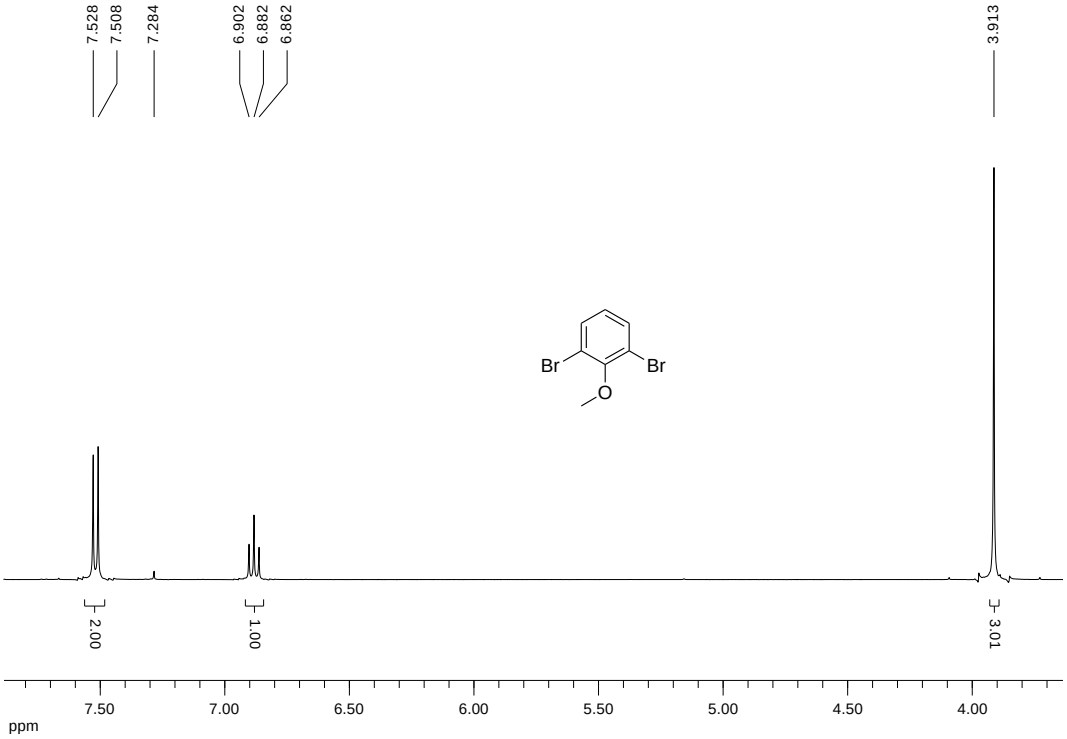
7.528
7.508
7.284
6.902
6.882
6.862
3.913
Br
Br
O
2.00
1.00
3.01
7.50
7.00
6.50
6.00
5.50
5.00
4.50
4.00
ppm

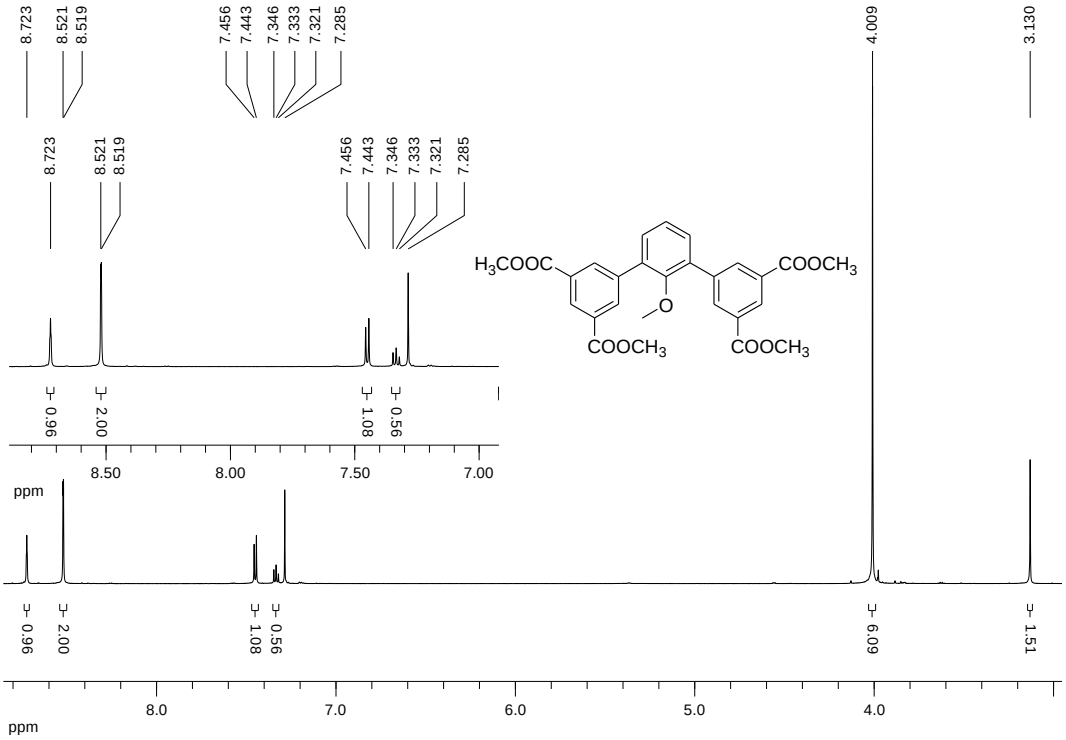
8.723
8.521
8.519
7.456
7.443
7.346
7.333
7.321
7.285
4.009
3.130
H3COOC
COOCH3
O
COOCH3
COOCH3
0.96
2.00
1.08
0.56
6.09
1.51
ppm

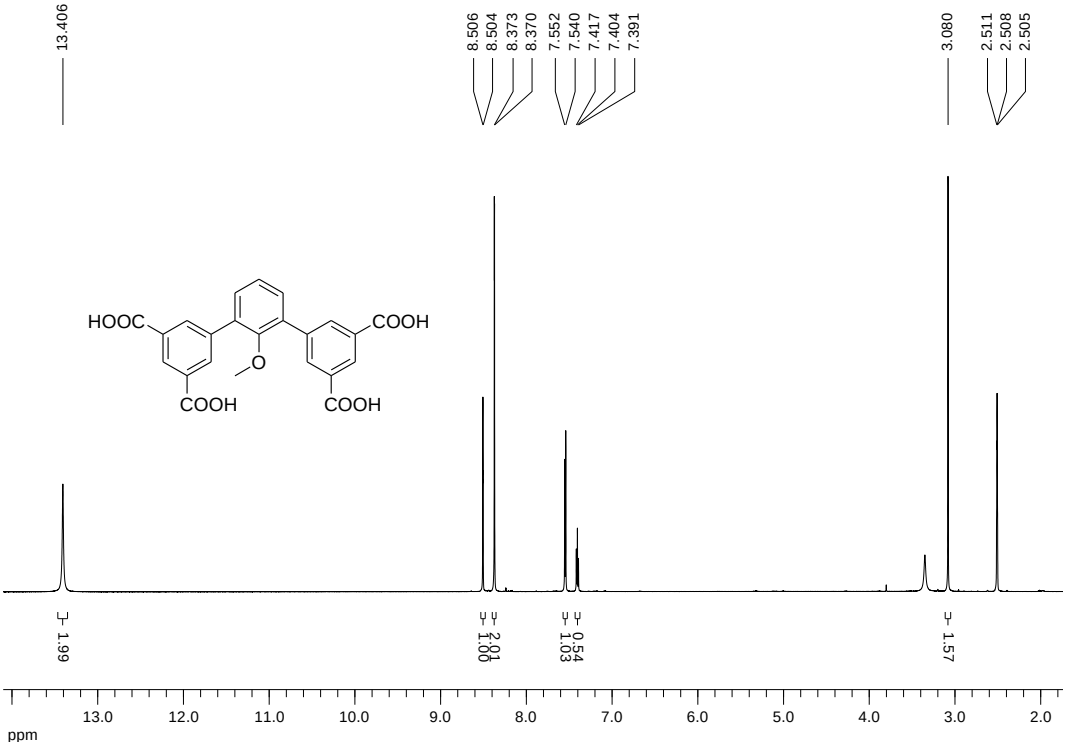
13.406
8.506
8.504
8.373
8.370
7.552
7.540
7.417
7.404
7.391
3.080
2.511
2.508
2.505
HOOC
COOH
O
COOH
COOH
COOH
1.99
2.01
1.00
0.54
1.03
1.57
ppm

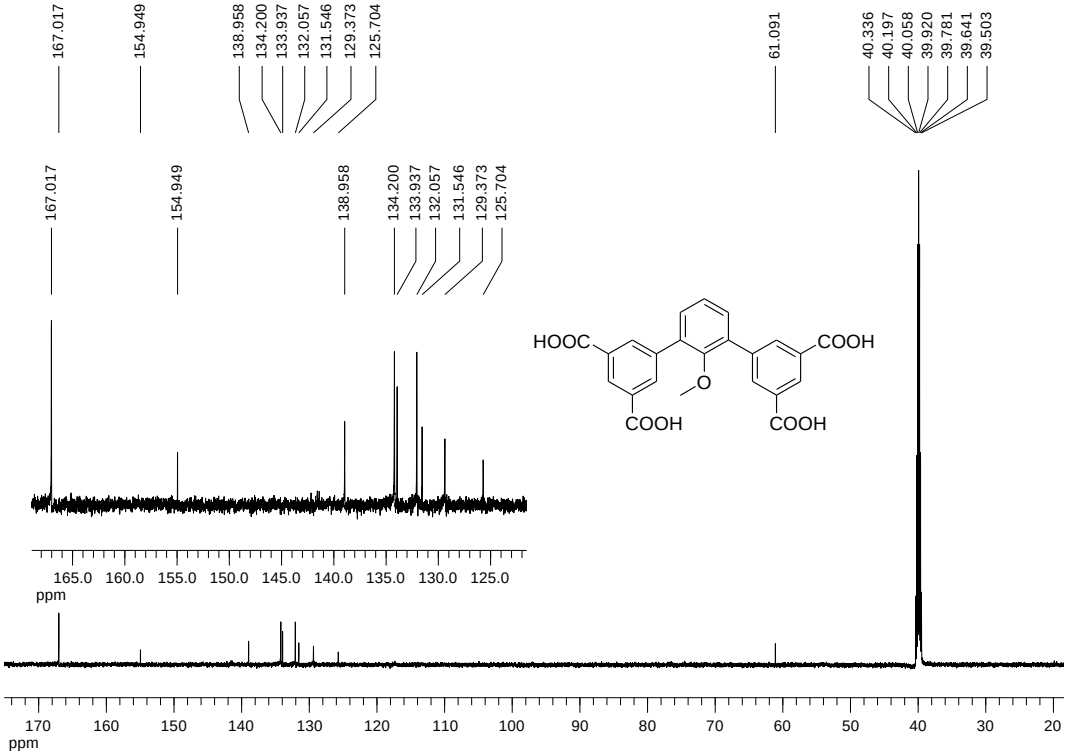
167.017
154.949
138.958
134.200
133.937
132.057
131.546
129.373
125.704
61.091
40.336
40.197
40.058
39.920
39.781
39.641
39.503
HOOC
COOH
O
COOH
COOH
ppm

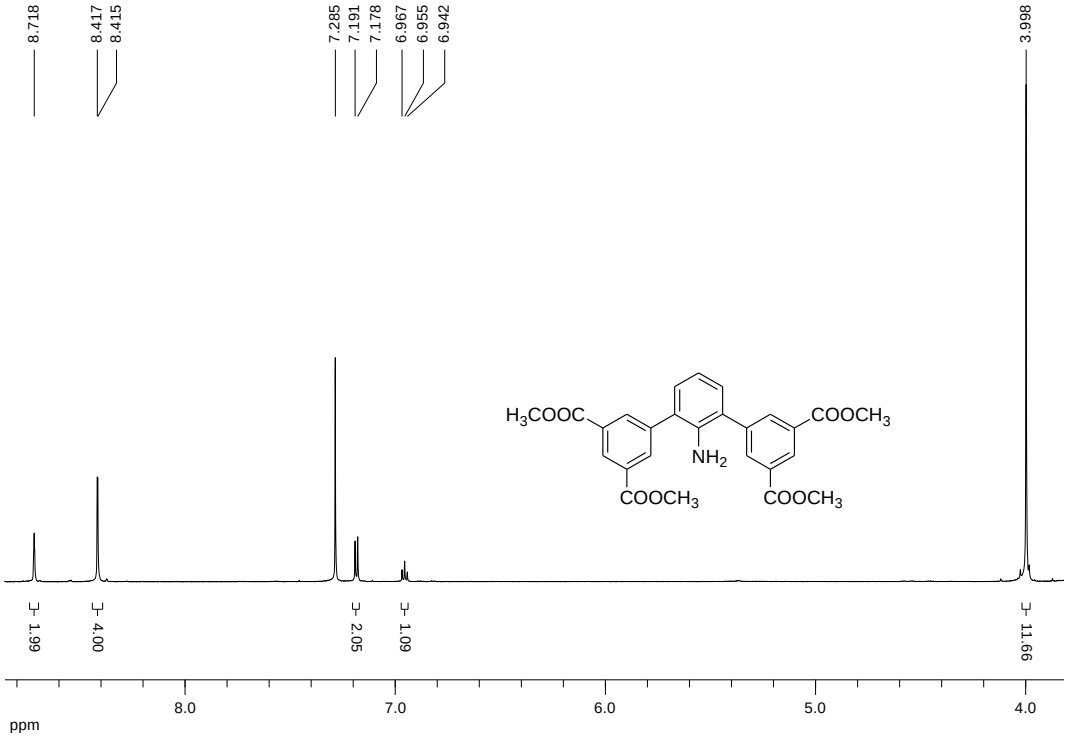
8.718
8.417
8.415
7.285
7.191
7.178
6.967
6.955
6.942
3.998
H3COOC
COOCH3
NH2
COOCH3
COOCH3
1.99
4.00
2.05
1.09
11.66
ppm

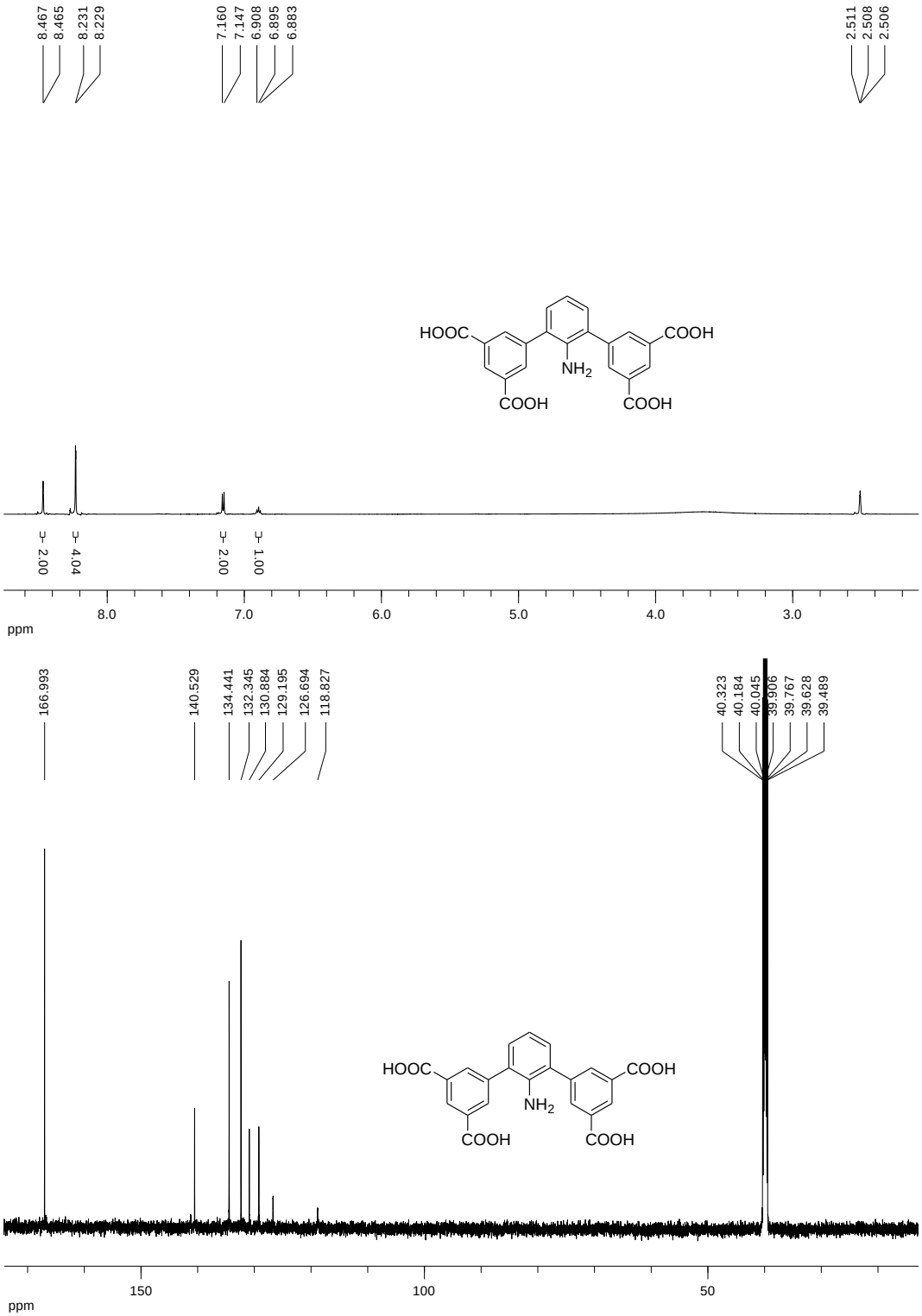

Fig. S21 ^{1}H and ^{13}C NMR spectra.

Table S1 Crystal data and structure refinement for **ZJNU-101**, **ZJNU-102**, and **ZJNU-103**.

MOFs	**ZJNU-101**	**ZJNU-102**	**ZJNU-103**
Empirical formula	$C_{40}H_{58}Cu_2N_6O_{17}$	$C_{44}H_{65}Cu_2N_7O_{18}$	$C_{37}H_{52}Cu_2N_6O_{16}$
Formula weight	1022.00	1107.11	963.95
λ (Å)	1.54178	0.71073	0.71073
Crystal system	Orthorhombic	Cubic	Hexagonal
Space group	*C*mc2(1)	*Pm-3*	$P6_3/mmc$
Unit cell dimensions	a = 24.9038(10) Å b = 33.4493(12) Å c = 18.3388(7) Å α = 90° β = 90° γ = 90°	a = 25.3148(4) Å b = 25.3148(4) Å c = 25.3148(4) Å α = 90° β = 90° γ = 90°	a = 18.5762(5) Å b = 18.5762(5) Å c = 23.8042(16) Å α = 90° β = 90° γ = 120°
V (Å^3)	15276.5(10)	16222.7(8)	7113.7(6)
Z	12	12	6
D_c (g cm^{-3})	1.333	1.360	1.350
μ (mm^{-1})	1.632	0.860	0.966
F(000)	6408	6960	3011
θ range for data collection (°)	2.212 to 66.489	2.276 to 28.279	2.673 to 24.994
Limiting indices	$-28 \le h \le 20$ $-39 \le k \le 39$ $-21 \le l \le 21$	$-33 \le h \le 21$ $-33 \le k \le 28$ $-30 \le l \le 28$	$-16 \le h \le 22$ $-22 \le k \le 22$ $-28 \le l \le 28$
Reflections collected / unique	30571 / 11714	50295 / 7179	74827 / 2361
R_{int}	0.0448	0.0640	0.0594
Refinement method	Full-matrix least-squares on F^2	Full-matrix least-squares on F^2	Full-matrix least-squares on F^2
Data/restraints/parameters	11714 / 1 / 466	7179 / 0 / 176	2361 / 8 / 86
Goodness-of-fit on F^2	1.004	1.021	1.089
Final R indices [$I > 2\sigma(I)$]	R_1 = 0.0447 wR_2 = 0.1253	R_1 = 0.1166 wR_2 = 0.3343	R_1 = 0.0941 wR_2 = 0.3623
R indices (all data)	R_1 = 0.0470 wR_2 = 0.1285	R_1 = 0.1470 wR_2 = 0.3882	R_1 = 0.1159 wR_2 = 0.4170
Largest diff. peak and hole (e·Å^{-3})	0.974 and -0.450	2.326 and -1.033	2.182 and -1.245
CCDC	1895248	1895249	1895250

Table S2 Langmuir-Freundich parameters for adsorption of C_2H_2, CO_2, and CH_4 in **ZJNU-101**.

Guest	q_{sat} (mmol g^{-1})	b_0 $(kPa)^{-v}$	E (kJ mol^{-1})	v	R^2
C_2H_2	20.56898	1.83018×10^{-5}	18.245	0.65466	0.99922
CO_2	21.01804	2.96428×10^{-7}	22.109	1	0.99997
CH_4	13.18114	1.6832×10^{-6}	14.953	1	0.99995

Table S3 Langmuir-Freundlich parameters for adsorption of C_2H_2, CO_2, and CH_4 in **ZJNU-102**.

Guest	q_{sat} (mmol g^{-1})	b_0 $(kPa)^{-v}$	E (kJ mol^{-1})	v	R^2
C_2H_2	14.00042	1.92974×10^{-5}	18.863	0.69987	0.99967
CO_2	14.88163	3.02368×10^{-7}	23.168	1	0.99976
CH_4	13.35692	1.39833×10^{-6}	15.289	1	0.99997

Table S4 Langmuir-Freundlich parameters for adsorption of C_2H_2, CO_2, and CH_4 in **ZJNU-103**.

Guest	q_{sat} (mmol g^{-1})	b_0 $(kPa)^{-v}$	E (kJ mol^{-1})	v	R^2
C_2H_2	14.60785	5.96129×10^{-6}	21.720	0.75546	0.99977
CO_2	17.14944	3.96943×10^{-7}	22.407	1	0.99976
CH_4	10.27678	1.18441×10^{-6}	16.689	1	0.99998

Table S5 Summaries of textural parameters (obtained from N_2 adsorption isotherms at 77 K) and gas adsorption properties of three MOFs investigated in this work.

MOFs	$S_{BET}/S_{Langmuir}$ ($m^2 g^{-1}$)	V_p ($cm^3 g^{-1}$)	D_c ($g\ cm^{-3}$)	C_2H_2 uptake [a] ($cm^3 g^{-1}$, STP)			CO_2 uptake [a] ($cm^3 g^{-1}$, STP)			CH_4 uptake [a] ($cm^3 g^{-1}$, STP)			C_2H_2/CH_4 IAST selectivity [a] (v/v = 1:1)			CO_2/CH_4 IAST selectivity [a] (v/v = 1:1)		
				298 K	288 K	278 K	298 K	288 K	278 K	298 K	288 K	278 K	298 K	288 K	278 K	298 K	288 K	278 K
ZJNU-101	2825/3087	1.101	0.690	173.5	204.9	238.7	90.8	115.6	147.0	20.6	25.2	30.6	31.5	35.3	40.4	5.27	5.88	6.66
ZJNU-102	2585/2902	1.041	0.687	157.7	180.1	203.3	91.0	113.6	139.2	19.9	24.4	29.9	30.0	32.6	36.1	5.86	6.58	7.46
ZJNU-103	2132/2502	0.894	0.762	184.5	209.8	233.9	101.3	128.4	156.0	22.2	27.4	34.0	36.2	42.3	51.0	6.01	6.66	7.48

[a] at 800 mmHg; S_{BET} = BET surface area; $S_{Langmuir}$ = Langmuir surface area; V_p = pore volume; D_c = framework density (without solvent molecules and terminal water molecules) derived from single-crystal X-ray structures;